UDC 533.6.013.14 : 629.1.025.3 https://doi.org/10.15407/itm2022.04.026

K. V. TERNOVA[1], G. O. STRELNIKOV[1], N. S. PRYADKO[1], M. O. KATRENKO[2]

THE INFLUENCE OF THE LENGTH OF SHORTENED NOZZLE WITH TIP ON TRACTION CHARACTERISTICS

[1]Institute of Technical Mechanics
of the National Academy of Sciences of Ukraine and the State Space Agency of Ukraine,
st. Leshko-Popelya, 15, 49005, Dnipro, Ukraine; e-mail:np-2006@ukr.net
[2]Oles Honchar Dnipro National University, Gagarin av. 72, 49010, Dnipro, Ukraine

В даний час при вирішенні нових завдань розробники сопла для ракетного двигуна все частіше звертаються до нетрадиційних конфігурацій, що відрізняються від класичного сопла Лаваля. Порівняно новим напрямом у проєктуванні надзвукових сопел є створення так званого дзвоноподібного сопла, яке має, на відміну від класичного сопла Лаваля, більший кут входу в надзвукову частину сопла. При цьому розглядаються сопла з двома ділянками розширення потоку надзвукової частини сопла. При вирішенні подібних завдань не розглядався вплив співвідношення довжин обох ділянок скороченого сопла на його характеристики. Метою даної роботи було визначення впливу довжини конічної початкової надзвукової ділянки з незмінною формою дзвоноподібного насадка на розподіл статичного тиску в соплі та його тягові характеристики.

При дослідженні показників цього сопла використовувався обчислювальний пакет ANSYS Fluent. В результаті досліджень було показано, що картини течії в соплі (поля швидкостей) змінюються зі зміною довжини вхідної (у насадок) конічної частини і ступеня недорозширення потоку. В земних умовах ($P_н$ = 1 бар) для всіх варіантів спостерігається розвинена відривна зона, що починається від кутової точки переходу конічної частини в насадок; при цьому тиск на стінці насадка практично дорівнює тиску навколишнього середовища. За великого ступеня недорозширення потоку в соплі (P_0 = 300) і в «порожнистих» умовах ($P_н$ =0,1 бар) потік у насадці примикає до стінки. При великому ступені недорозширення потоку в соплі тиск у насадці зростає від кутової точки до зрізу насадка, а зі зменшенням довжини насадка тиск на зрізі насадка збільшується. Коефіцієнт тяги сопла зменшується зі збільшенням ступеня недорозширення потоку в соплі, досягаючи постійного значення після примикання потоку до стінки насадка за кутовою точкою переходу сопла в насадок. При великих ступенях недорозширення потоку коефіцієнт тяги сопла вище для сопла з більшою довжиною конічної частини. Результати розрахунків добре корелюють з результатами експериментальних досліджень подібних сопел.

Ключові слова: *скорочене сопло ракетного двигуна, дзвоноподібний насадок, розподіл швидкостей у потоці, розподіл статичного тиску в соплі, коефіцієнт тяги сопла*.

Nowadays, for solving new problems, rocket engine nozzle developers are increasingly turning to nontraditional nozzle configurations that differ from the classic Laval one. A relatively new line in the design of supersonic nozzles is the development of the so-called bell-shaped nozzle, which, unlike the classical Laval nozzle, has a larger angle of entry into the supersonic part of the nozzle. In this case, dual bell nozzles, which have two flow expansion sections in their supersonic part, are considered. However, the effect of the length ratio of the two flow expansion sections of a truncated nozzle on its characteristics has not yet been studied. The goal of this work is to determine the effect of the length of the upstream conical supersonic section on the static pressure distribution in the nozzle and its thrust characteristics with the shape of the bell-shaped tip kept unchanged. .

The nozzle characteristics were studied using the ANSYS Fluent computing package. It was shown that the flow patterns in the nozzle (velocity fields) change with the length of the conical part upstream of the tip and the underexpansion degree. Under terrestrial conditions ($P_н$ = 1 bar), all variants show a developed separation zone that starts from the corner point where the tip is connected to the conical part. In this case, the pressure on the nozzle wall is nearly equal to the ambient pressure. At a large flow underexpansion degree (P_0 = 300 bar) and in low-pressure conditions conditions ($P_н$ =0.1 bar), the flow in the tip is adjacent to the wall. At a large flow underexpansion degree, the pressure in the nozzle increases from the corner point to the tip exit, and the pressure at the tip exit increases with decreasing tip length. The nozzle thrust coefficient decreases with increasing flow underexpansion degree, and it reaches a constant value after the flow becomes adjacent to the tip wall downstream of the corner point where the tip is connected to the nozzle. At high flow underexpansion degrees, the nozzle thrust coefficient is higher for a nozzle with a longer conical part. The calculated results are in good agreement with experimental data on nozzles of this type.

Keywords: *truncated supersonic nozzle, bell-shaped tip, static pressure distribution in nozzle, flow velocity distribution, nozzle thrust coefficient.*

Introduction. At present, when solving new tasks, rocket engine nozzle designers are increasingly turning to unconventional configurations that differ from the classic Laval nozzle.

Nozzles of minimum length and various shapes were investigated with the use

of the characteristic method [1 – 3]. It was shown that for the shortened nozzle wave thrust losses increase in it, caused with low-intensity shock waves and local separation zones in the nozzle.

A relatively new direction in the design of supersonic nozzles is the creation of the so-called bell-shaped nozzle, which, unlike the classic Laval nozzle, has a larger entry angle into the supersonic part of the nozzle [4 – 6].

Dual-Bell type nozzles [7, 8] with two bell-shaped sections are also considered. They are more efficient under conditions of changing flight altitude. Such a nozzle adapts to height and has two modes of operation. The study [8] revealed the influence of the nozzle geometry on the flow behavior and, as a result, on the efficiency of the nozzle.

For such nozzles, the method of characteristics no longer allows to detail all the features of a complex flow in a bell-shaped nozzle. In this case, the Computational Fluid Dynamics models (CFD) are more preferred [7, 9].

In [10], a shortened Laval nozzle with a spherical bell-shaped tip was studied. Unlike the Dual-Bell type nozzle, its first section is a conical Laval nozzle, and the second section is bell-shaped tip. Such a nozzle can be used in the development of compacted layouts of rockets [4]. At the same time, the advantages of the operation of such a nozzle with a change in flight altitude are retained. The characteristics of this nozzle were studied using the ANSYS Fluent software package [11]. The solution of the problem was verified with the results of experimental tests of such nozzles, presented in [12]

Previous researchers have not considered the influence of the length ratio of both sections of the bell-shaped nozzle on its characteristics was not considered.

In this work, the authors study the effect of the length ratio of the conical initial supersonic section and the bell-shaped tip.

The purpose of the work is to investigate the effect of the length changing of the conical initial supersonic section with the unchanged shape of the bell-shaped tip on the distribution of static pressure in the nozzle and its thrust characteristics.

Main part. The studies are carried out on the base model (Fig. 1) similar to the model № 6 used in the papers [12, 13], where : l – length of the conical shortened part of the nozzle; L – total length of the shortened nozzle with a tip;

d_a – the diameter of the conical part end; α – the half-angle of the opening of the conical part; α_t – tip entry angle.

In the present study, the length of the conical inlet of the Laval nozzle was varied. In this case, the total length of the nozzle L was changed with some unchanged parameters: the nozzle radius (R = 28 mm), the diameter of the critical section of the nozzle (d_{cr} = 10 mm) and the entrance diameter of the inlet part (d_a = 16 mm). The geometrical parameters of the studied variants (1 – 4) of short nozzles with a bell-shaped nozzle are shown in Table 1 below with the same designations as in Fig. 1.

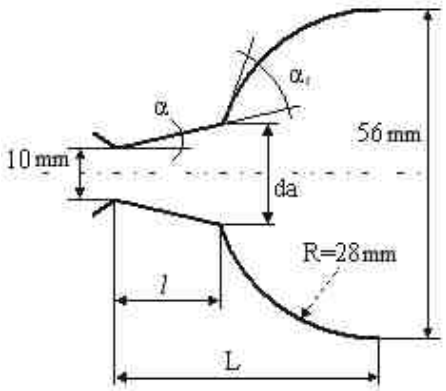

Fig. 1 – Geometric parameters of the shortened nozzle

Table 1 – Geometric parameters of the studied nozzle variants

variant	l, mm	L,mm	α, *deg*	α_t, *deg*	d_a, mm
1	5	30	30	45	16
2	10	35	20	55	16
3	15	40	11	64	16
4	20	45	8	67	16

The calculations are carried out using the ANSYS Fluent package. The boundary and initial conditions, as well as the turbulence model, are chosen similarly to previously published papers [10, 13].

Figure 2 shows the distribution of flow velocities in the nozzle with a nozzle variant 1 (Fig. 2, a)) and 4 (Fig. 2, b)) at an external pressure of $P_н$ = 1 bar and pressure at the nozzle inlet P_0= 50 bar.

In both cases, the flow at the outlet of the shortened nozzle separates from the tip wall at the corner point of transition of the nozzle conical part into the tip spherical part. With a smaller length of the conical part (Fig. 2, a)), a larger diameter and a shorter length of the first “barrel” are observed due to the larger half-opening angle (α) of the conical part. In this case, the flow from the ambient into the region between the tip wall and the jet boundary adjoins the tip wall with a developed vortex structure at the tip wall and at the free boundary of the flow. A toroidal vortex is formed on the end section of variant 1 nozzle (Fig. 2, a)), the scale of which is smaller than for variant № 4 (Fig. 2, b)), where the vortex near the wall spreads from the tip end to the corner point. In the conical part of both nozzle variants, the pressure gradients differ and are determined by the half-angle of the shortened part. The subsonic velocities of the vortex structure in both cases determine the pressure on the tip wall, which is approximately equal to the ambient pressure (for more details, see below).

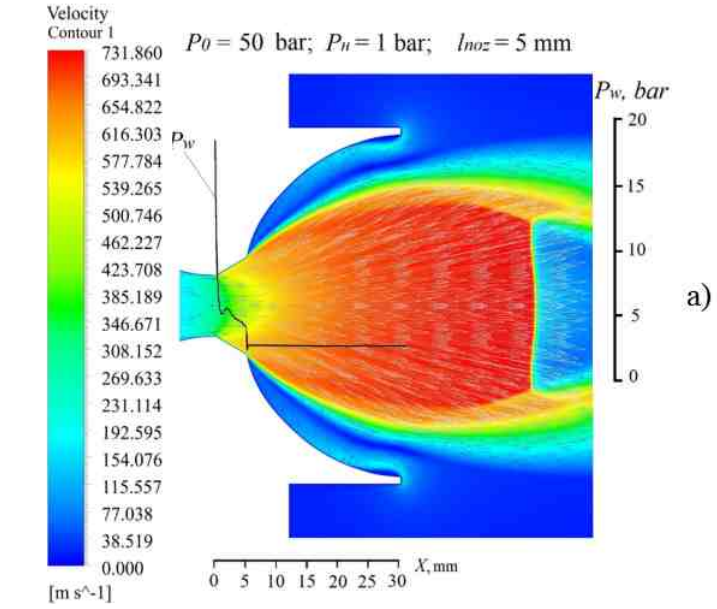

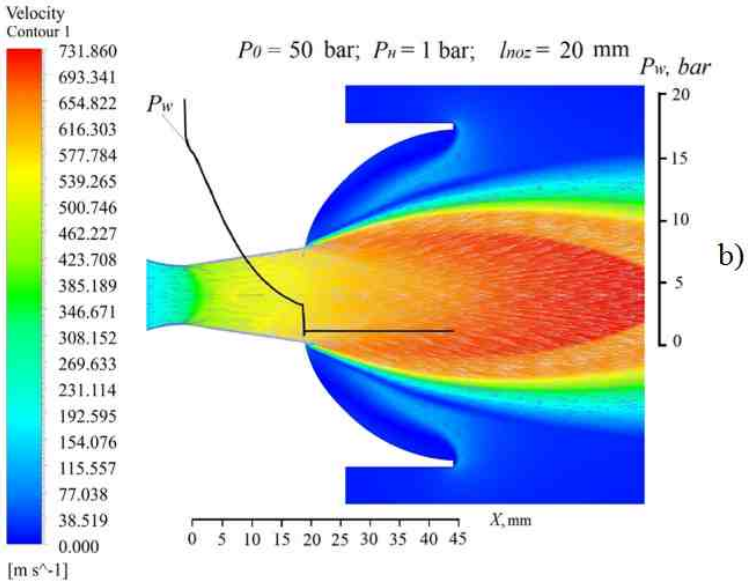

variants: a – № 1, b – № 4 and pressure on the wall (P_w) at P_0=50 bar

Fig. 2 – Distributions of flow velocities in the nozzle with a tip

At a high inlet flow pressure P_0 = 300 bar (Fig. 3)), the jet boundary adjoins the tip wall in both variants (1 and 4).

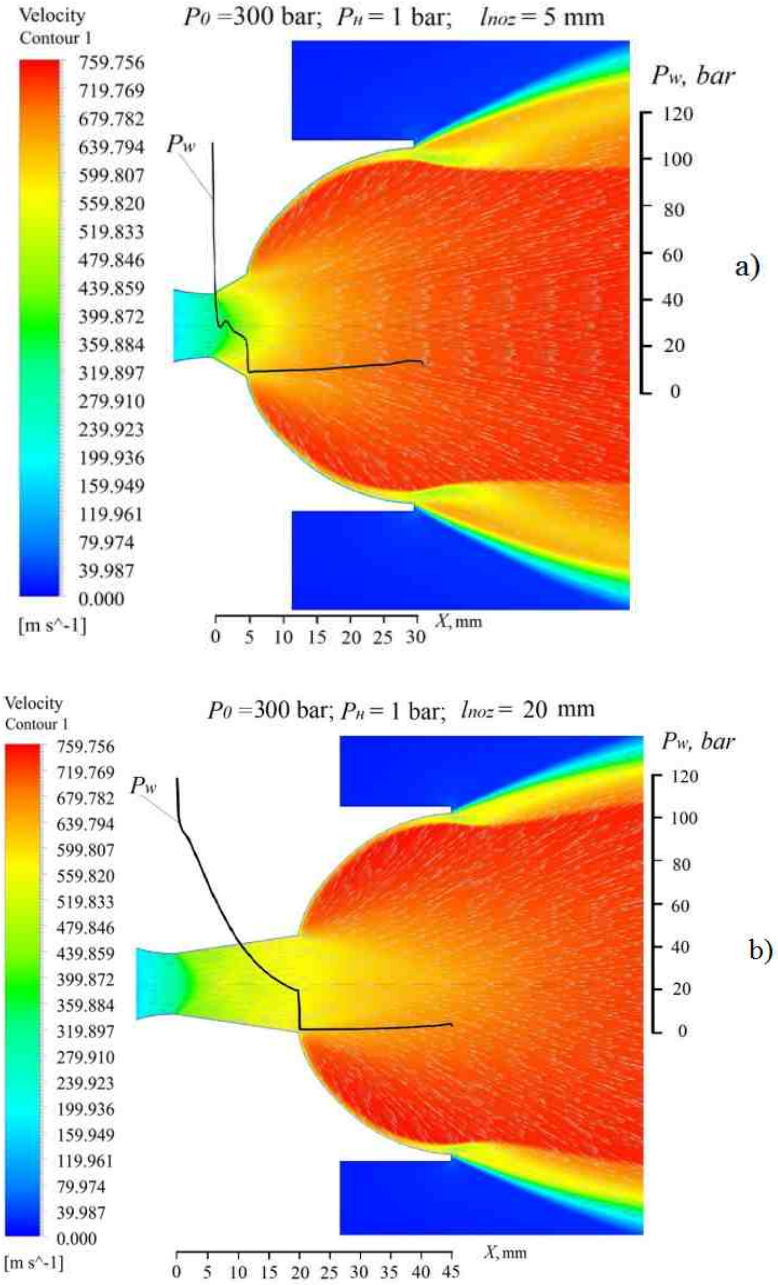

variants: a – № 1, b – № 4 and pressure on the wall (P_w) at P_0 = 300 bar

Fig. 3 – Distribution of flow velocities in the nozzle with a tip

With a smaller length of the conical part (variant 1 in Fig. 3, a)), due to the larger half-opening angle of the inlet conical part, a hanging shock in front of the tip wall of greater intensity is observed behind the tip end compared to variant 4 (Fig. 3, b)), which causes the formation of a more expanded (greater jet opening angle) of the flow structure behind the nozzle end. Qualitatively, the character of the change in the static pressure in the nozzle is similar to the character at a lower inlet pressure (Fig. 2)). More detailed quantitative estimates of the distribution of static pressure are carried out below.

The change in the pressure of the external ambient as well as the degree of non-design flow in the nozzle ($N = P_0 / P_w$) significantly affects the flow pattern in the nozzle and behind the nozzle. The behavior of the flow in a nozzle with nozzles in "empty" conditions is studied – at an external pressure of $P_н$ = 0.1 bar. Figure 4 shows the distributions of velocity (Fig. 4, a)) and flow density (Fig. 4, b)) in a nozzle with a tip (variant № 1) at P_0 = 50 bar.

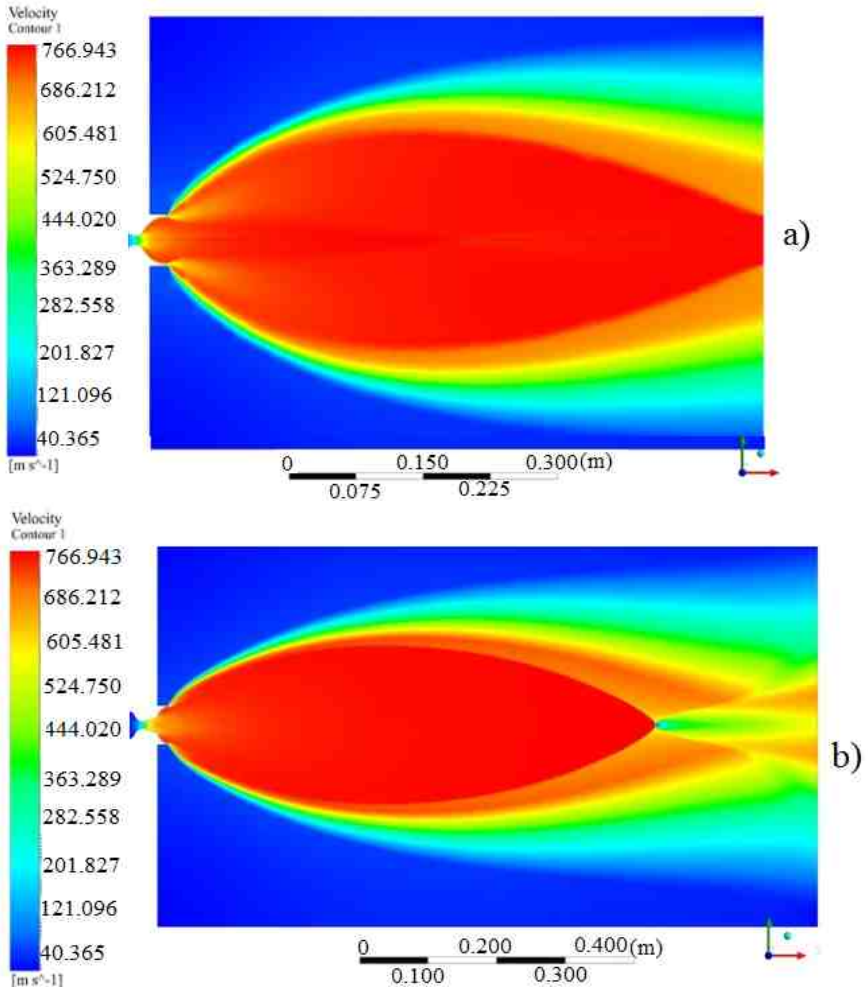

variants: a – № 1, b – № 4 at P_0 = 50 bar and $P_н$ = 0.1 bar

Fig. 4 – Distribution of flow velocities in the nozzle with a tip

As it can be seen, the flow pattern (Fig. 4, a)) is similar to the flow pattern at P_0 = 300 bar (Fig. 3, a)). However, the opening angle of the jet behind the nozzle end is larger than at $P_н$ = 1 bar. The first “barrel” of the Mach flow structure has an extended character with a slightly expressed Mach disk (Fig. 4, a)). For a longer nozzle (Fig. 4, b)), the length of the first “barrel” is shorter with almost the same diameter.

Below, we consider the features of static pressure distribution in the nozzle with a tip (variants № 1 – Fig. 5, a), 5, c), and variants № 4 Fig. 5, b), 5, d) at an external outlet pressure $P_н$ = 1 bar and an inlet pressure P_0 = 50 bar (Fig. 5, a), 5, b) and P_0 = 300 bar (Fig. 5, c), 5, d)).

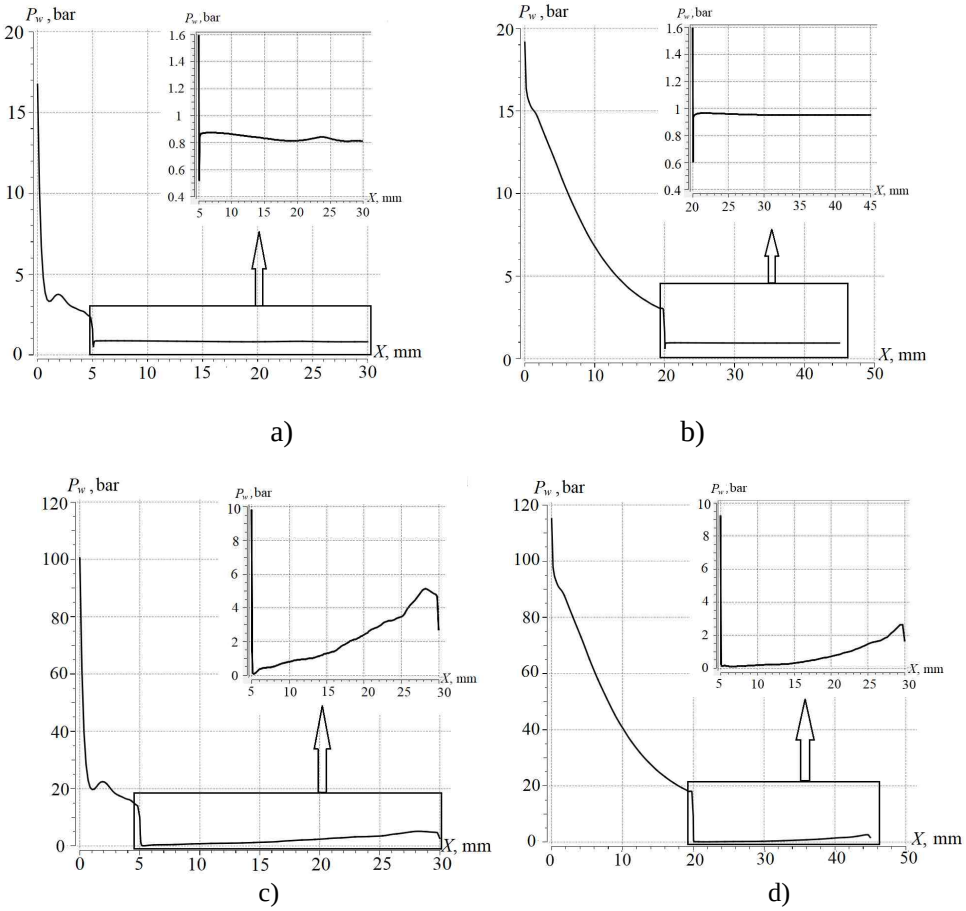

a) P_0 = 50 bar; l = 5 mm, b) P_0 = 50 bar; l = 20 mm; c) P_0 = 300 bar; l = 5 mm; d) P_0 =300 bar; l = 20 mm

Fig. 5 – Distribution of static pressure in the nozzle of variant № 1 (a, c) and variant № 4 (b, d) at $P_н$ = 1 bar

At P_0 = 50 bar, the pressure in the nozzle with a short conical part (variant № 1, Fig. 5, a)) is less than for the variant with a longer part (variant № 4, Fig. 5, b)). At the same time, for variant № 4, the pressure is almost constant along the entire length of the tip (0.96 bar), while for variant № 1 the pressure is not constant and ranges from 0.9 to 0.8 bar (at the nozzle end). This is caused by the above-mentioned inflow of the external flow to the tip wall and the formation of a local vortex at its end. The pressure distribution in the shortened conical part is characterized by a different gradient and the presence of a local pressure increase at the inlet to the conical section (Fig. 5, a)), which is explained by the large half-opening angle of the wall of the conical part.

With a large underexpansion of the flow in the nozzle (N = 300), the pressure in the nozzle behind the corner point increases in both variants (Fig. 5, c) – variant 1, Fig. 5, d) – variant 4), having the same character of change along the length of the tip. With a short length of the nozzle (variant № 1, Fig. 5, c)) the pressure rises to the end up to 5 bar and for variant № 4 (Fig. 5, d)) the pressure rises to 3 bar. At the nozzle exit, a pressure drop occurs, caused by the acceleration of the expanding flow in the boundary layer at the tip exit (Fig. 2).

At low external pressure (in “empty” conditions, $P_н$ =0.1 bar), the character of pressure change in the nozzle is similar to the character of pressure change in case of large underexpansion of the flow (in “terrestrial” conditions, $P_н$ =1 bar). In this case, the pressure at the nozzle section of variant № 1 (1.35 bar, Fig. 6, a)) is also higher compared to variant № 4 (0.7 bar, Fig. 6, b)). At the same time, the pressure at the nozzle section differs almost twice for variants № 1 and № 4 at different external ($P_н$ =1 bar, Fig. 5 and $P_н$ =0.1 bar, Fig. 6) and inlet pressures (P_0 = 300 bar Fig. 5, c)), 5, d) and P_0 = 50 bar Fig. 6).

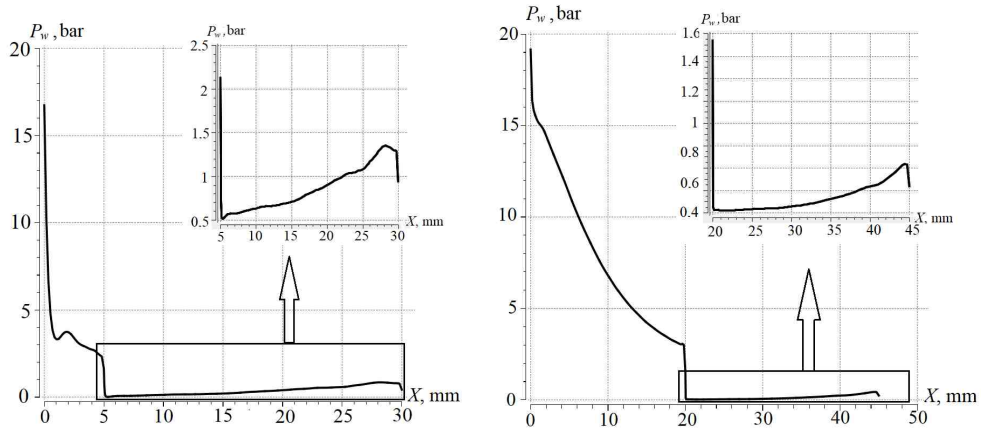

Fig. 6 – Distribution of static pressure in the nozzle of variant № 1 (a) and variant № 4 at $P_н$ = 0.1 bar; P_0 = 50 bar

Flow calculations in the nozzle with a tip were carried out for all 4 variants (see Table 1).

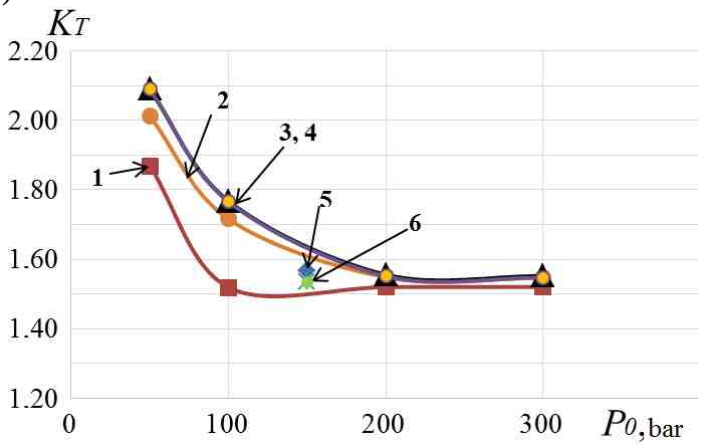

l: 1 – 5 mm; 2 – 10 mm; 3 – 15 mm; 4 – 20 mm; 5 – experiment at l = 15 mm (model №3 [12]); 6 – experiment at l = 10 mm (model №6 [12])

Fig. 7 – Dependence of the nozzle thrust coefficient on the pressure in front of the nozzle at $P_н$ = 1 bar

The efficiency of a nozzle is determined by its thrust coefficient ($K_т$). The dependence of the thrust coefficient on the pressure at the nozzle inlet has the same character with a decrease in the length of the conical part of the nozzle (Fig. 7). With an increase in the degree of non-design flow in the nozzle, the thrust coefficient decreases to an approximately constant value after the flow past the corner point to the tip wall. With the length of the conical part l = 5 mm (variant № 1),

this occurs when $P_0 \approx 100$ bar. For variant № 2 – № 4, this occurs at $P_0 \approx 200$ bar. After that, the thrust coefficient remains almost constant. The thrust coefficient for variant № 1 is the smallest and amounts to ~ 1.5. For variants № 2 – 4, this value is ~ 1.6. The experimental values of the thrust coefficient obtained in [12] are in good agreement with the calculated values (Fig. 7): at l = 15 mm, the value is $K_т$ = 1.566; at l = 10 mm – $K_т$= 1.536.

Conclusions. It is shown that the patterns of flow in the nozzle (velocity fields) change with a change in the length of the inlet (into the nozzles) conical part and the degree of non-design flow.

Under terrestrial conditions ($P_н$ = 1 bar), for all variants, a developed separation zone is observed, starting from the corner point of the transition of the conical part into the tips. For this case, the pressure on the tip wall is practically equal to the ambient pressure. With a large degree of flow underexpansion in the nozzle (N = 300) and in "empty" conditions ($P_н$ =0.1 bar), the flow in the tip adjoins the wall. With a large degree of non-design flow in the nozzle, the pressure increases in the tip from the corner point to the nozzle exit, and with a decrease in nozzle length, the pressure increases at the tip exit.

The nozzle thrust coefficient ($K_т$) decreases with an increase in the degree of flow non-design in the nozzle, reaching a constant value after the flow adjoins the tip wall behind the corner point of the transition of the nozzle into the tip. At high degrees of non-design flow, $K_т$ is higher for a nozzle with a longer conical part. The calculation results correlate well with the results of experimental studies of such nozzles.

1. *Kumar A., Ogalapur S. G.* Design of minimum length nozzle by method of characteristics. International Journal of Science, Engineering and Technology. 2020. No. 8(6). Pp. 1–7.
2. *Özkan Yu. E.* Design of a supersonic nozzle using method of chacteristics. Graduation project. Department of Astronautical Engineering. Istanbul Technical University. Faculty of Aeronautics and Astronautics. 2021. 37 pp.
3. *Murnaghan M.* Study of minimum length, supersonic nozzle design using the method of characteristics. Master's Thesis. Escola Superior d'Enginyeries Industrial, Aeroespacial i Audiovisual de Terrassa (ESEIAAT). Terrassa, June 2019. 82 pp.
4. *Kovalenko N. D., Strelnikov G. A., Gora Yu. V., Grebenyuk L. Z.* Gas Dynamics of Truncated Supersonic Nozzles. Kyiv: Naukova Dumka, 1993. 223 pp. (in Russian).
5. *Joshi P., Gandhi T., Parveen S.* Critical designing and flow analysis of various nozzles using CFD analysis. International Journal of Engineering, Research & Technology. 2020. V. 9. Iss. 02. 2020. Pp. 421–424. https://doi.org/10.17577/IJERTV9IS020208
6. *Asha G., Mohana D. N., Priyanka K. S., Govardhan D.* Design of minimum length nozzle using method of characteristics. International Journal of Engineering Research & Technology (IJERT).2021. V. 10, Iss. 05. Pp. 490–495.
7. *Sreenath K.R, Mubarak A.K.* Design and analysis of contour bell nozzle and comparison with dual bell nozzle. International Journal of Engineering Research & Technology (IJERT). 2016. V. 3. Iss. 6. Pp. 52–56.
8. *Génin C., Schneider D., Stark.* R. Dual-bell nozzle design. Notes on Numerical Fluid Mechanics and Multidisciplinary Design. 2021. V. 146. Pp. 395–406. https://doi.org/10.1007/978-3-030-53847-7_25
9. *Krushna B., Srinivasa R. P., Balakrishna B.* Analysis of dual bell rocket nozzle using computational fluid dynamics. International Journal of Engineering Research & Technology (IJERT). 2013. V. 02. Iss. 11. Pp. 412–417. https://doi.org/10.15623/ijret.2013.0211060
10. *Ihnatiev O. D., Pryadko N. S., Strelnikov G. O., Ternova K. V.* Gas flow in a truncated Laval nozzle with a bell-shaped tip. Teh. Meh. 2022. No. 2. Pp. 39–46. https://doi.org/10.15407/itm2022.02.039
11. *Stolarski T., Nakasone Y., Yoshimoto S*. Engineering Analysis with ANSYS Software. 2nd Edition. Butterworth-Heinemann. 2018. 553 pp.
12. *Strelnikov G.A.* Adjustable Supersonic Nozzles of Small Length. Dnepropetrovsk: DGU Publishers, 1993. 191 pp. (in Russian).
13. *Ihnatiev O. D., Pryadko N. S., Strelnikov G. O., Ternova K. V.* Thrust characteristics of a truncated Laval nozzle with a bell-shaped tip. Teh. Meh. 2022. No. 3. Pp. 35–46. https://doi.org/10.15407/itm2022.03.035

Received on October 26, 2022,
in final form on November 18, 2022